IET Nanobiotechnology

*Research Article*

IET Journals
The Institution of Engineering and Technology

# Silver nanoparticles biosynthesised using *Centella asiatica* leaf extract: apoptosis induction in MCF-7 breast cancer cell line

ISSN 1751-8741
Received on 22nd February 2018
Revised 23rd April 2018
Accepted on 20th June 2018
E-First on 22nd August 2018
doi: 10.1049/iet-nbt.2018.5069
www.ietdl.org

*Shima Edalat Fard[1], Farzaneh Tafvizi[1] ✉, Maryam Bikhof Torbati[2]*

*[1]Department of Biology, Parand Branch, Islamic Azad University, Parand, Iran*
*[2]Department of Biology, College of Science, Yadegar-e-Imam Khomeini (RAH), Shahr-e-Rey Branch, Islamic Azad University, Tehran, Iran*
✉ *E-mail: farzanehtafvizi54@gmail.com*

**Abstract:** The aim of this study was to green synthesised silver nanoparticles (AgNPs) using *Centella asiatica* leaf extract and investigate the cytotoxic and apoptosis-inducing effects of these nanoparticles in MCF-7 breast cancer cell line. The characteristics and morphology of the green synthesised AgNPs were evaluated using transmission electron microscopy, scanning electron microscopy, UV–visible spectroscopy, X-ray diffraction, and Fourier-transform infrared spectroscopy. The MTT assay was used to investigate the anti-proliferative activity of biosynthesised nanoparticles in MCF-7 cells. Apoptosis test was performed using flow cytometry and expression of caspase 3 and 9 genes. The spherical AgNPs with an average size of 19.17 nm were synthesised. The results showed that biosynthesised AgNPs exhibited cytotoxicity, anti-cancer, apoptosis induction, and increased expression of genes encoding for caspases 3 and 9 in MCF-7 cancer cells in a concentration- and time-dependent manner. It seems that green synthesised AgNPs have potential uses for pharmaceutical industries.

## 1 Introduction

*Centella asiatica* (L.) Urban (*C. asiatica*) is a member of the Apiaceae family (Umbelliferae). It is an herbaceous, stable, and scalloped plant found in the semi-arid regions. Since ancient times, the plant has been known as the miraculous elixir of life [1, 2]. It is a native plant that is widely distributed in the tropical regions of both the hemispheres, especially in Sri Lanka and South Africa, Southeast Asia, Iran, India, some parts of China, and the Southwest of the sea of Iceland, Madagascar, the South and South-East of the United States, Mexico, Venezuela, and Colombia [3]. The earlier studies and some other reliable sources indicate that this herb is not found beyond the Anzali wetland area in Iran [4]. The plant contains medically useful compounds, including asiatic acid, madecassic acid, and other derivatives of triterpene ester glycosides, such as asiaticoside, sceffoleoside, and madecassoid. It also contains triterpene glycosides, such as centellasaponin, alkaloids, volatile and flavonoid compounds, steroids, and phenolic acid [5–8]. According to previous studies, *C. asiatica* extract has been shown to inhibit the growth of breast cancer cells in the culture medium [9–11]. Breast cancer is the most common cancer among women with an incidence of one in every 8–10 women. According to the statistics in Iran, one in every 10–15 women suffers from the risk of developing breast cancer. However, the incidence age of breast cancer in Iranian women is at least one decade less than that of women in developed countries. The average age of breast cancer diagnosis in western countries is 56 years, while in Iran, it is 45 years. Currently, the treatment modality of breast cancer involves surgery, chemotherapy, and radiotherapy. However, all of these suffer from the limitation of developing hypoxia at different levels. For instance, performing chemotherapy, with surgery to a lesser extent, leads to hypoxia and possibly cell death, ultimately causing damage to the healthy non-cancerous cells [12]. Nanotechnology is referred to as a branch of engineering that deals with the identification and control of materials in the range of 1–100 nm, thereby conferring unusual physical, chemical, and biological properties to nanoparticles, which in turn provide new and unique applications [13]. Silver nanoparticles (AgNPs) have important applications, including medical diagnostics [14, 15], drug transport [16], therapeutics, anti-oxidants [17], anti-bacterial [18] and cytotoxic [19] properties. AgNPs are produced via two methods: physico-chemical and biological methods [20]. The chemical methods of preparation of nanoparticles typically lead to the toxic reactants on nanoparticles. Thus, the use of plants as sustainable and available sources to obtain biocompatible nanoparticles has attracted many researchers in recent years [21].

In recent years, the use of plant extracts for the preparation of metal nanoparticles has been proposed as an easy and a suitable alternative over chemical and physical methods, especially the plant leaf extracts are most suitable for the synthesis of nanoparticles. Secondary metabolites, enzymes, proteins, and other reducing agents play a key role in the production of metal nanoparticles by plants [22].

The advantages of the method of green synthesised, as a way of synthesis of nanoparticles, include lower cost, eco-compatibility, and easy synthesis in large quantities. In this method, the use of high temperature and high pressure, as well as chemical capping, reduction, and stabilising agents for the synthesis of nanoparticles are not required. In addition, in the biosynthesis method, the binding of some of the compounds present in the plant extract during synthesis to the surface of the nanoparticles produced modifies and improves the activities of nanoparticles [23]. Recently, many studies have reported the potential power of plant-derived nanoparticles to control the growth of tumour cells accompanied by an improved cytotoxic effect owing to the presence of secondary metabolites and other non-metallic compounds in the reaction environment [24]. The anti-proliferative effect of *C. asiatica* extract on MCF-7 breast cancer cells has been shown in previous studies. However, cytotoxic effects, induction of apoptosis, and the expression of the intrinsic apoptosis pathway genes, including caspases 3 and 9, by green synthesised AgNPs in the MCF-7 cell line of breast cancer have not yet been studied and are being reported for the first time in this study.

## 2 Methods

### *2.1 Extraction and green synthesised of nanoparticles*

The plant, *C. asiatica*, was collected from the areas of Bandar Anzali wetland during spring and was confirmed by the botanical experts at the Islamic Azad University. Fresh leaves washed several times with water. Then the leaves were air-dried and ground to a powdered form. The dried powder of *C. asiatica* leaves

was utilised for the extraction by addition of 20 g of the powdered plant to 500 ml of ethanol, followed by an incubation at an ambient temperature for 24 h on a shaker. The resulting extract was filtered using a filter paper. A sedimentation method, based on the reduction of silver ions ($AgNO_3$; Merck, Germany) by *C. asiatica* extract, was used to synthesise AgNPs with high purity. For the synthesis of AgNPs, 100 ml of 0.01 mM aqueous solution of silver nitrate (EMD Millipore, Billerica, MA, USA) was mixed with 4 ml of the plant extract, and the mixture was continuously stirred for 5 min at room temperature. The mixture was kept undisturbed until the colourless solution turned dark brown, revealing the reduction process of Ag + to Ag0 NPs. The particles were then separated out by centrifugation at 13,000 rpm for 20 min. Then, the biosynthesised AgNPs were dried at 37°C for 4 h.

### 2.2 Structure confirmation of nanoparticles

*2.2.1 UV–visible spectroscopic characterisation of AgNPs:* The spectroscopic analysis of AgNPs synthesised using *C. asiatica* extract was performed using a UV–Vis Perkin Elmer device in the range of 200–800 nm.

*2.2.2 X-ray diffraction (XRD) analysis:* Crystallographic structures of the green synthesised AgNPs were performed by XRD method. XRD test was carried out with Cu Ka radiation in the range of $2\theta = 10°–80°$.

*2.2.3 Fourier-transform infrared (FT-IR) spectroscopic studies:* FT-IR spectroscopy studies were performed using a spectrum RX 1 instrument. The FT-IR spectra were scanned between 4000 and 400 $cm^{-1}$ at a resolution of 4 $cm^{-1}$ in the transmittance mode.

*2.2.4 Field-emission scanning electron microscopy (FE-SEM) and transmission electron microscopy (TEM):* Morphological studies and size examination of the synthesised AgNPs were conducted by a FE-SEM (FE-SEM, SIGMA; Carl Zeiss Meditec AG; Jena, Germany) and a TEM (Leo 906, Zeiss100 KV model, Germany).

### 2.3 Cytotoxicity assays and in vitro anti-cancer activity

*2.3.1 Cell line and cell culture:* In this study, the MCF-7 human breast adenocarcinoma cell line (IBRC C10682) was provided by the Iranian Biological Resource Center (IBRC). The MCF-7 cell line was cultured in RPMI 1640 medium containing 10% foetal bovine serum (FBS), 1% penicillin–streptomycin at 37°C in a humid atmosphere with 5% $CO_2$. To study morphology, health and the number, the cells were checked using an inverted microscope. When the cells reached at least 70% cell growth, they were detached from the bottom of the flask by 0.05% trypsin and centrifuged at 1500 rpm for 5 min. The resulting precipitate was produced as suspension and the percentage of living cells was determined by Neubauer chamber and Trypan blue dye by optical microscopy. After ensuring no contamination, cells with viability above 90% were used for the investigation.

*2.3.2 MTT assay and cell viability:* MTT test was used to evaluate the cytotoxic effect of MCF-7 cells. A 100 µl culture medium containing 10,000 MCF-7 cells were seeded into 96-well plates separately and incubated for 24 h. Then different concentrations of AgNPs (3, 5, 12.5, 25, 50 and 100 µg/ml) were added to the wells separately and the plates were incubated for 24 and 48 h. Then, 100 µl of MTT (3,4,5-dimethylthiazolyl-2)−2,5-diphenyltetrazolium bromide (Sigma, Germany) was added to each well at 0.5 mg/ml concentration, and they were incubated for 4 h at 37°C in a humidified incubator with a 5% $CO_2$ environment. The purple crystals of formazan formed in cell cytoplasm were dissolved by adding pure DMSO solution to the wells. Optical absorbance was determined using an ELISA reader at 570 nm. The results were reported as viability percentage and $IC_{50}$ value.

*2.3.3 Apoptosis/necrosis assay by Annexin V-FITC:* Evaluation of apoptosis induction was performed in accordance with the Annexin V-FITC kit (eBioscience, USA Affymetrix,). For this purpose, MCF-7 cells were treated with 5, 8.76 ($IC_{50}$ concentration) and 12.5 µg/ml of AgNPs for 24 h. The cellular analysis was performed by flow cytometry device (Biocompare, USA).

*2.3.4 Analysis of apoptosis-related gene expression (caspase 3 and 9):* At first, MCF-7 cells were treated with 5, 8.76 µg/ml ($IC_{50}$ concentration) and 12.5 µg/ml of AgNPs for 24 h and 3, 5 µg/ml (IC50 concentration) and 12.5 µg/ml for 48 h. RNA extraction and cDNA synthesis were performed according to CinnaGen (Iran) and Revert AidTM First Strand cDNA Synthesis Kits (Fermentas) protocols, respectively. Briefly, the cells were lysed by RNX solution (Trizol reagent) (200 µl of chloroform was added to 1 ml of RNX solution). Samples were centrifuged at 12,000 rpm. Then three phases were formed. The RNA molecule was placed in the upper phase and the protein and DNA were placed in the middle and lower phases. The high transparent phase was transferred to the new vial. A volume of isopropanol the same as the supernatant phase volume was added then centrifuged for 15 min at 12,000 rpm. The supernatant was discarded and the pellet was dissolved in DEPC water. After confirming the quality and quantity of RNA, cDNA synthesis was performed according to the protocol of the Revert AidTM First Strand cDNA Synthesis Kit (Fermentas, Germany). In summary, 1–2 µg of the RNA, 1 µl of DNAse and 1 µl of 10 × buffer were mixed and incubated at 37°C for 30 min. 1 µl of EDTA was added and incubated at 65°C for 10 min to inactivate the DNAse enzyme activity. Then, 4 µl of 5 × buffer, 0.5 µl of RNasin (40 unit/µl), 2 µl of dNTP mixture (10 mM), 2 µl of dT oligo, 1.5 µl of $MgCl_2$, and 1 µl of Reverse Transcriptase (RT) enzyme were added. The reaction mixture was placed in a thermocycler for 60 min at 42°C. Samples were put in a thermocycler for 10 min at 70°C to deactivate RT enzyme. The reaction product was kept at −20°C. SYBER Green method was used to determine the expression of caspase 3 and 9 genes in MCF-7 cells treated with AgNPs after 24 h and 48. The beta-actin gene was used as internal control. The final volume of each reaction was considered 25 µl as follows; 12.5 µl of Mater mix (Bioneer, Korea), (0.1–1 µg) 1 µl of synthesised cDNA of β-actin, caspase 3 and 9 genes, (10 mM) 1 µl of forward and reverse primers for each gene (Takapuzist company), 9.5 µl of DEPC water. The sequence of primers is presented in Table 1. The polymerase chain reaction (PCR) for each gene was performed separately and repeated three times. The real-time PCR was performed with the Bioneer exicycler 96 according to the following protocol. The temperature program was optimised as follows; pre-denaturation at 95°C for 10 min; 40 cycles of denaturation at 95°C for 20 s, annealing at 57°C for 40 s and extension at 72°C for 40 s. After the reaction, data was extracted from the device as Ct and gene expression was measured using a ΔΔCt method by Rest software. Then, the gene expression was plotted using the SPSS version 19 and Graph pad software.

### 2.4 Statistical analysis

Statistical analysis was performed using SPSS 19 software (SPSS Inc., Chicago, IL, USA) and the results were analysed by one way ANOVA. The expression level of target genes between the treated samples and control group was measured by Tukey's HSD post-hoc test. Data were presented as the mean ± standard deviation (SD) and $P<0.05$ considered as statistically significant.

## 3 Results

### 3.1 Biosynthesis of AgNPs using C. asiatica

The synthesis of AgNPs was first confirmed by the change in the colour of the solution from transparent to yellow. The colour then turned brown due to the reduction of silver ions and their accumulation as AgNPs.

**Table 1** Specific primer sequences used for real-time PCR

| Genes | Primer sequence |
|---|---|
| ***Caspase3*** | Forward: 5′-ACATGGCGTGTCATAAAATACC-3′ |
| | Revers: 5′-CACAAAGCGACTGGATGAAC-3′ |
| ***Caspase9*** | Forward: 5′-CATATGATCGAGGACATCCAG-3 |
| | Revers: 5′-TTAGTTCGCAGAAACGAAGC-3′ |
| ***GAPDH*** | Forward: 5′-TCTCTGATTTGGTCGTATTGG-3′ |
| | Revers: 5′-GAATCATATTGGAACATGTAAACC-3′ |

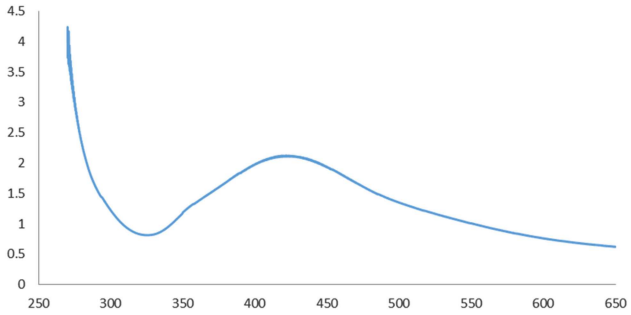


**Fig. 1** *UV–vis absorption spectrum of biosynthesised AgNPs using C. asiatica extract*

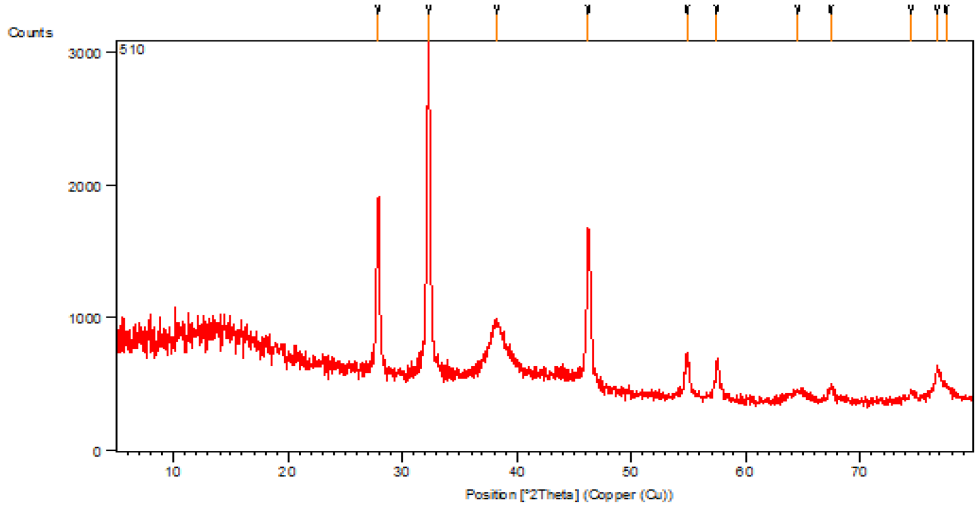


**Fig. 2** *XRD patterns of biosynthesised AgNPs using the C. asiatica extract*

### *3.2 UV–vis spectroscopic analysis*

The absorption peak at 430 nm in the UV–vis absorption spectrum of AgNPs synthesised using *C. asiatica* extract confirmed their synthesis (Fig. 1). The appearance of this peak could be attributed to the surface plasmon resonance (SPR) of AgNPs.

### *3.3 XRD analysis*

The XRD patterns of AgNPs are presented in Fig. 2. The X-ray patterns showed diffraction peaks at 2 of about 38.26, 46.24, 64.54, and 77.49° corresponding to (111), (200), (220), and (311) planes of the face-centred cubic (fcc) silver crystal, respectively.

### *3.4 FTIR spectroscopy analysis*

The analysis of the FTIR spectrum of the *C. asiatica* extract showed the presence of various biomolecules. The presence of a broad and strong peak (13,413 $cm^{-1}$) in the spectrum was related to the stretching vibrations of O–H alcohol and phenolic groups in the extracts. The absorption peak at 2926 $cm^{-1}$ belonged to the tensile vibrations of the C–H groups of aliphatic groups. A strong absorption peak at 1617 $cm^{-1}$, associated with tensile vibrations of C = O bond, was indicative of a carbonyl amide group of the protein. The C–O–C phenolic tensile vibration peak at 1271 $cm^{-1}$ and tensile vibration peaks of C–O–C and C–O–H alcohols at 1070 $cm^{-1}$ along with a few peaks that were very close to it were visible only at higher frequencies. The bending vibrations of the C–H bonds of C = C–H groups were seen in the region below 1000 $cm^{-1}$ (Fig. 3*a*). The spectrum of AgNPs reduced by the plant extract exhibited considerably high similarities with the spectrum of the extracted juice, implying that the extraction process was well performed. The O–H peak shift from 3413 to 3429 $cm^{-1}$ was attributed to the binding of O–H groups to AgNPs. The reduction in the absorbance frequency of the stretching vibration of the carbonyl amide group from 1617 to 1615 $cm^{-1}$ indicated the binding of silver to this group. Groups, such as hydroxyl, amide, and carbonyl, in the plant extract, are likely to contribute to the biological reduction of Ag to AgNPs (Fig. 3*b*).

### *3.5 TEM and SEM analysis*

The SEM image analysis revealed that the synthesised nanoparticles have a spherical structure and a size ranging from 20 to 60 nm. The TEM and SEM images are shown in Figs. 4*a* and *b*. The average diameter of the nanoparticles synthesised was measured to be 19.17 nm. The histogram of the size of the nanoparticles is presented in Fig. 4*c*.

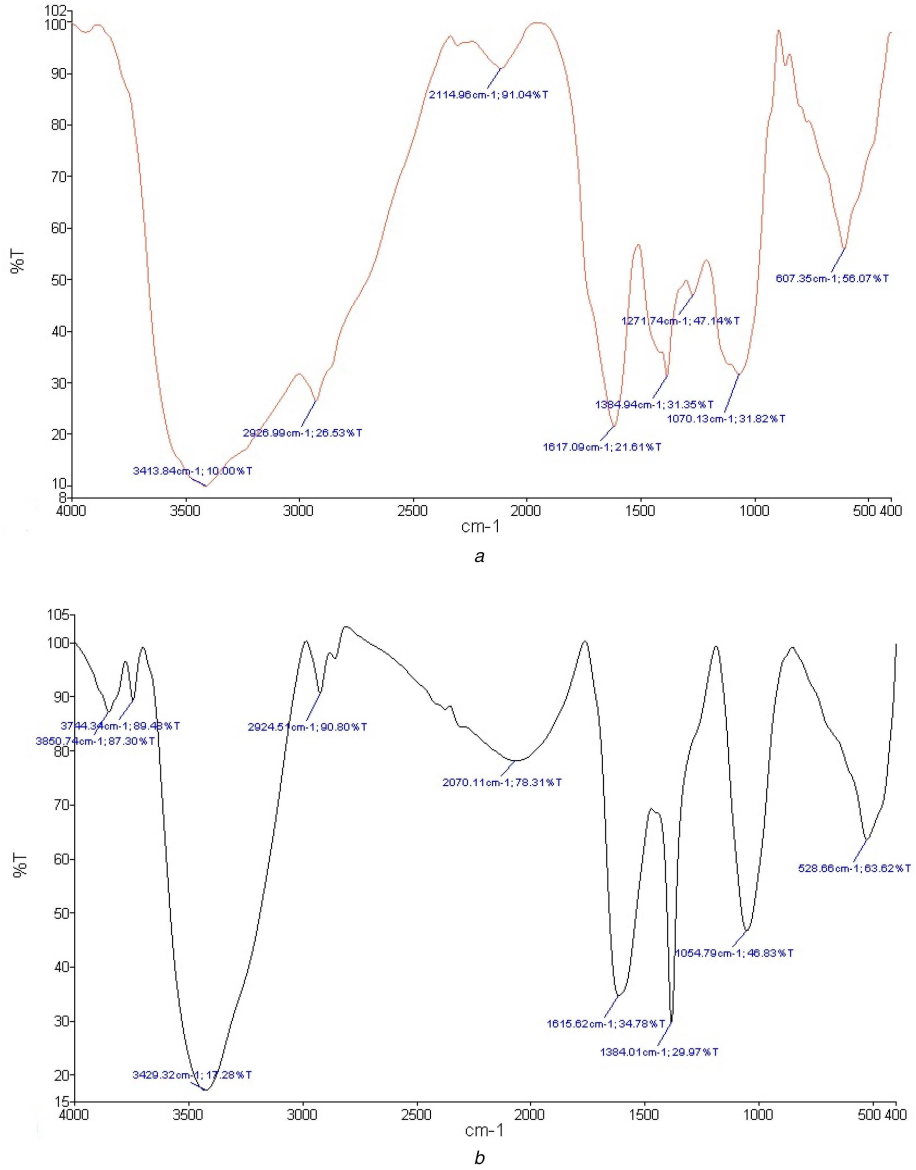


**Fig. 3** *FT-IR spectra*
***(a)*** FT-IR of *C. asiatica* leaf extract ***(b)*** FT-IR of Biosynthesised nanoparticles

### *3.6 Cell viability analysis*

The MCF-7 cells were treated with 3.0, 5.0, 12.5, 25.0, 50.0, and 100.0 µg/ml of biological nanoparticles for 24 and 48 h. The results showed that AgNPs had the highest inhibitory effect at 100 µg/ml, which was statistically significant compared to the control group ($P$<0.001). However, the concentration of 3 µg/ml displayed the least anti-proliferative activity. The $IC_{50}$ values of the nanoparticles after 24 and 48 h of treatment on the MCF-7 cell line were 8.76 and 5.0 µg/ml, respectively. These results clearly demonstrated the cytotoxic effect of nanoparticles synthesised by cancer cells to be dependent on the time and dose of the nanoparticles. The results of the MTT test and induction of cytotoxicity are presented in Fig. 5.

### *3.7 Induction of apoptosis in MCF-7 cells treated with nanosilver particles synthesised using plant extract*

During the programed cell death or apoptosis, phosphatidylserine is transferred from the inner surface to the outer surface of the cell membrane. Apoptosis can be detected using Annexin dye, which, after binding to phosphatidylserine on the extracellular surface, is identified by flow cytometry. Also, propidium iodide (PI) is attached to the fragmented DNA of the nuclei of dead cells and is detectable by a flow cytometry device. The MCF-7 cancer cells were treated with 5.0, 8.76, and 12.5 µg/ml concentrations of nanoparticles for 24 h. The untreated cells were considered as the control group.

Flow cytometry results are shown in Fig. 6. At all three concentrations, the rate of early apoptosis in MCF-7 cells increased significantly compared to the control group. The highest apoptosis was observed at the $IC_{50}$ value of nanoparticles compared to the control group, which was statistically significant ($P$<0.001) (Table 2). The rate of late apoptosis was also found to increase at all three concentrations in comparison with the control group ($P$<0.001). An increase in the 22% primary apoptosis and 10% in late apoptosis was observed at $IC_{50}$ of the nanoparticles, as compared to the untreated cells (Table 2). In another analysis, the total percentage of cells placed in the Q1 and Q2 regions was considered as the percentage of total apoptosis (old and young apoptotic cells) and compared with cells located in the Q4 region (representing necrotised cells). The apoptotic cells were three-fold higher than the necrotic cells at all three concentrations (5.0, 8.76, and 12.5 µg/ml, $P$<0.001) (Table 3). The highest induction of apoptosis was observed at $IC_{50}$ (8.76 µg/ml) of the biological nanoparticle.

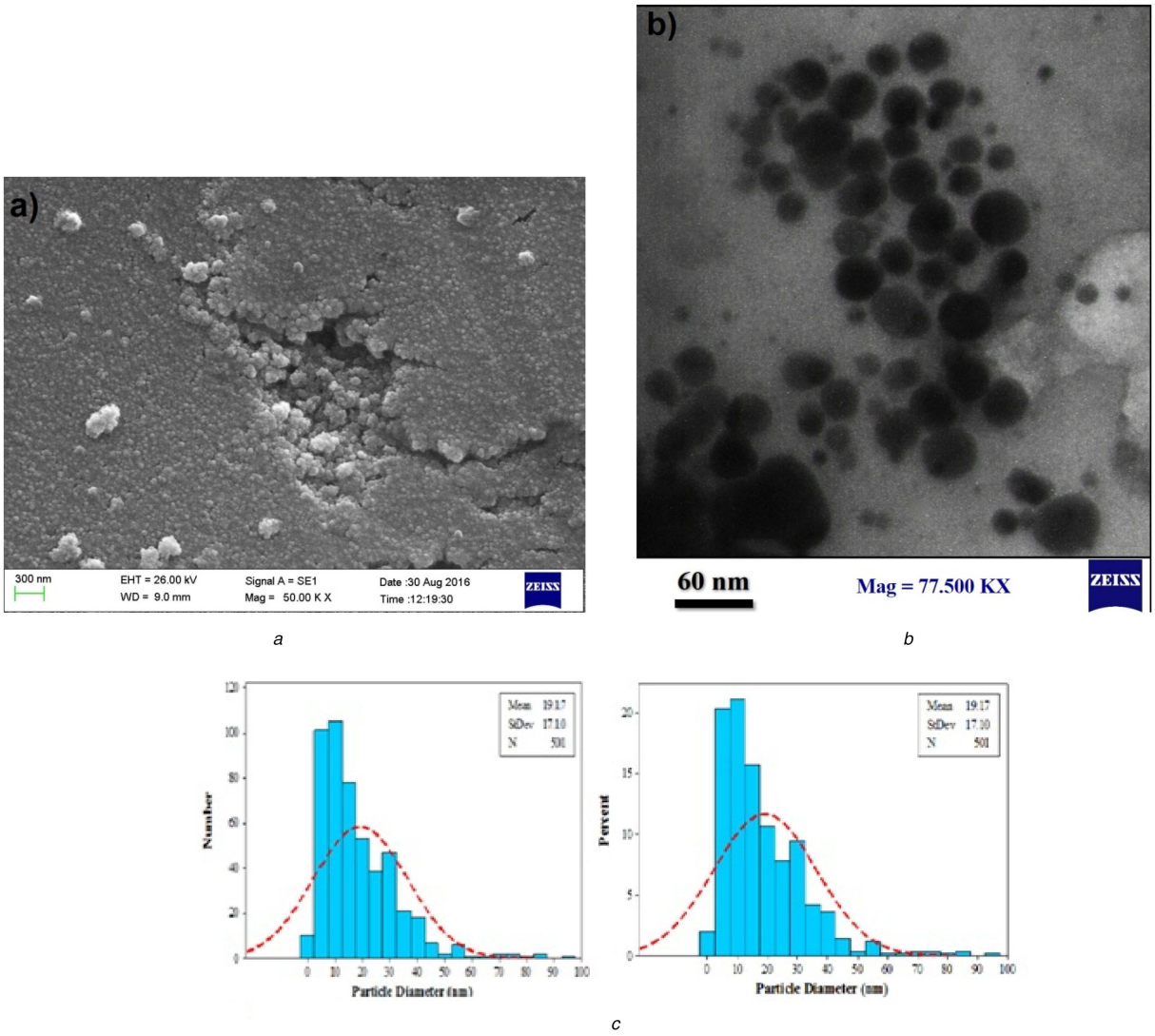


**Fig. 4** *Electron microscopy analysis of biosynthesised AgNPs*
***(a)*** SEM micrograph of biosynthesised AgNPs, ***(b)*** TEM micrograph of biosynthesised AgNPs, ***(c)*** Particle size distribution histogram of synthesised AgNPs using *C. asiatica* extract

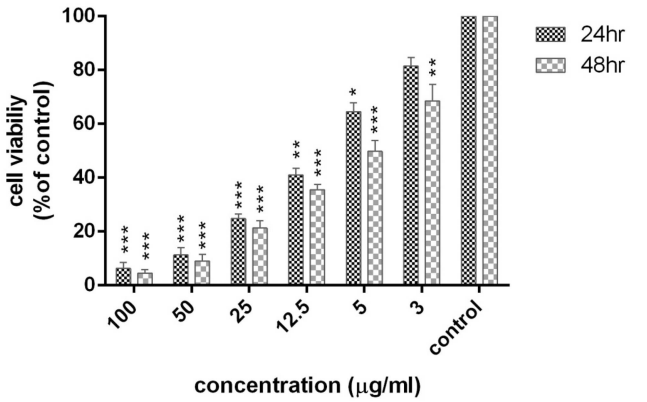


**Fig. 5** *Results of the MTT assay in MCF-7 cells treated with biological nanoparticles after 24 and 48 h (results are reported as viability in comparison with control samples) [p≤0.001: ***, p≤0.01:**, p≤0.05:*] (n = 3)*

### *3.8 Expression of caspase 3 and 9 genes in MCF-7 cells treated with biosynthesised AgNPs*

To test the expression of caspase 3 and 9 genes in MCF-7 cells, 5.0 μg/ml, $IC_{50}$ (8.76 μg/ml) and 12.5 μg/ml concentrations of the synthesised nanoparticles after 24 h and 3.0 μg/ml, $IC_{50}$ (5.0 μg/ml), and 12.5 μg/ml concentrations after 72 h were used. All concentrations led to an increase in the expression of caspases 3 and 9 genes in MCF-7 cancer cells compared to the control group. The highest increase in the mRNA levels of the genes was observed at the $IC_{50}$ concentration of nanoparticles after 24 and 48 h. A higher degree of expression was observed at 24 h than at 48 h (Figs. 7 and 8). The mRNA levels of caspase 3 and 9 genes at $IC_{50}$ (8.76 μg/ml) of nanoparticles were more than those at 5.0 μg/ml in 24 h ($P$<0.01) (Fig. 8*a*). In addition, at $IC_{50}$ (5.0 μg/ml) of nanoparticles at 48 h, a significant increase was observed in the expression of both genes compared to 3.0 μg/ml after 48 h ($P$<0.001) (Fig. 8*b*).

## 4 Discussion

Considering the growing importance of protecting the environment in recent years, the development of green techniques for the synthesis of nanoparticles is of paramount significance. For this purpose, bacteria, fungi, and plant extracts have been utilised to synthesise AgNPs. Among these, plants serve as good bioreductant for the synthesis of nanoparticles owing to the presence of several chemical constituents in the plant extracts [25].

The mechanism of synthesis of nanoparticles (AgNPs) using plant extract is not completely understood. Probably, the factors, such as alkaloids, glycosides, flavonoids, amino acids, phenolic compounds, saccharides, and tannins, are involved in this mechanism, which can reduce Ag metal into AgNPs [26].

AgNPs, by interacting with the membrane proteins and activating signalling pathways, inhibit cell growth. These nanoparticles can also be taken into the cells, either by diffusion or endocytosis, and can concentrate inside mitochondria, where they

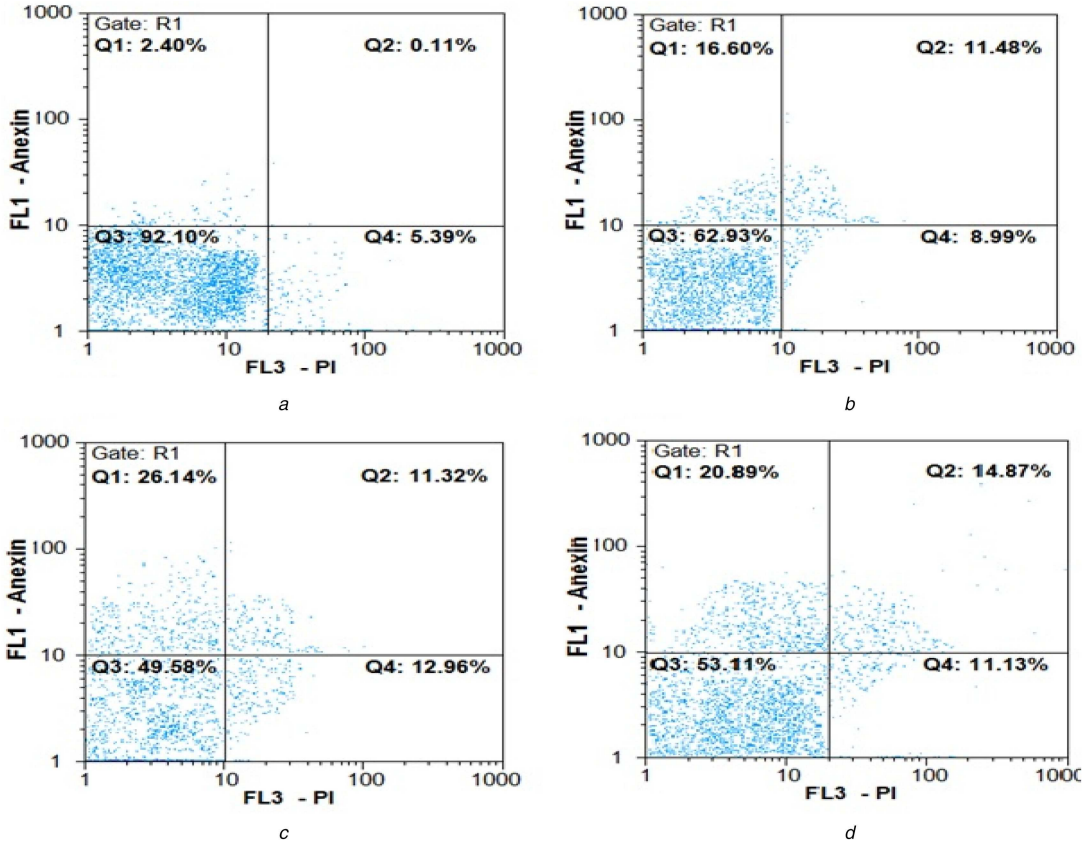


**Fig. 6** *Flow cytometry chart for evaluating apoptosis induced by AgNPs in 24 h*

***(a)*** Control cells (untreated cells), ***(b)–(d)*** 5, 8.76 µg/ml ($IC_{50}$ value) and 12.5 µg/ml of green synthesised AgNPs, respectively. *Q*1 represents early apoptotic cells with Annexin-FITC + and $PI^-$ staining index, *Q*2 represents late apoptotic cells with Annexin-FITC + and PI +, *Q*3 represents healthy cells with Annexin-$FITC^-$ and $PI^-$ staining index and *Q*4 is necrotic cells with Annexin-$FITC^-$ and PI + staining index

**Table 2** Apoptosis induced by AgNPs synthesised using *C. asiatica* extract

| | Control | 5 µg/ml | *P* value | IC50 (8.76 µg/ml) | *P* value | 12.5 µg/ml | *P* value |
|---|---|---|---|---|---|---|---|
| early apoptosis | 3.31 ± 0.7 | 16.46 ± 0.7 | <0.001 | 25.23 ± 0.5 | <0.001 | 21 ± 0.3 | <0.001 |
| late apoptosis | 0.88 ± 0.8 | 11.13 ± 0.9 | <0.001 | 10.22 ± 0.4 | <0.001 | 14.72 ± 0.1 | <0.001 |
| necrosis | 4.67 ± 0.9 | 8.78 ± 1.2 | 0.08 | 10.23 ± 0.6 | <0.05 | 11.39 ± 0.2 | <0.05 |

**Table 3** Comparison of apoptotic and necrotic cells at IC50 of the phytosynthesised AgNPs

| | 5 µg/ml | IC50 (8.76 µg/ml) | 12.5 µg/ml |
|---|---|---|---|
| apoptotic cells | 27.59 | 35.45 | 35.72 |
| necrotic cells | 8.78 | 10.23 | 11.39 |
| *P* value | <0.001 | <0.001 | <0.001 |

cause mitochondrial dysfunction and activate apoptosis. Oxidative stress occurs when reactive oxygen species (ROS) levels exceed the capacity of the antioxidant defence system. AgNPs regulate the activation of ROS, consequently damaging proteins and nucleic acids within the cell [27–30].

One of the most important toxic effects of AgNPs is their interaction with sulphur-containing molecules (such as proteins) due to the high affinity of silver for sulphur. It is well known that AgNPs can interact with proteins and amino acids. The amino acids, such as cysteine, have been widely used as surface-coating agents for nanosilver particles. It is believed that the interaction of AgNPs with proteins is an important mechanism that contributes to the toxicity of these nanoparticles, as Saptarshi *et al.* found that nanoparticles caused alterations in proteins, particularly their unfolding and change in function [31].

AgNPs are also able to bind to DNA and interact with it to cause structural changes in it, thereby resulting in DNA damage [32]. AgNPs can be absorbed by a variety of cells. It has been shown that the absorption of AgNPs depends on the size and shape of nanoparticles and time. Lu *et al.* [33] showed that spherical and rod-shaped nanoparticles can be absorbed into human keratinocytes in a time-dependent manner.

AgNPs in the mitochondria cause disturbance and inhibition of cellular respiration, leading to the expression of genes encoding for caspases 3 and 9. This, in turn, causes the cell cycle to progress to apoptosis. Since cellular respiration in cancer cells is critical and performed at a much higher rate than normal cells, its prevention or disruption rapidly leads the cells to apoptosis [25].

Hsin *et al.* [34] demonstrated that AgNPs causes the release of cytochrome C into the cytosol and promotes the transfer of BAX into the mitochondria. Further, AgNPs induce apoptosis through the mitochondrial pathway by activation of ROS and JNK in NIH3T3 fibroblast cells. The interaction of nanosilver particles with DNA was also demonstrated as evident by the arresting of the cell cycle in the G2/M phase.

In this study, *C. asiatica* leaf extract was utilised to synthesise biological AgNPs followed by an investigation of the effects of cytotoxicity and anti-cancer of green synthesised AgNPs in MCF-7 cell line. The results showed that AgNPs can exert the highest inhibitory effect at a concentration of 100.0 µg/ml on cell

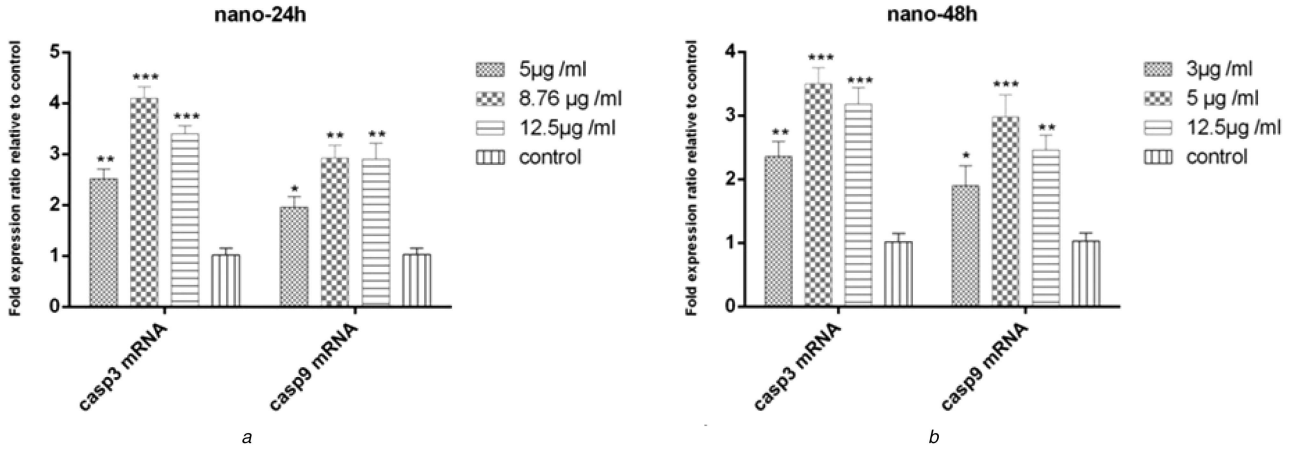


**Fig. 7** *Expression levels of caspase 3 and 9 genes*
***(a)*** After 24 h of treatment with biosynthesised nanoparticles in the MCF-7 cell line ***(b)*** after 48 h (results are reported as fold expression comparison with control samples) [$p \leq 0.001$:***, $p \leq 0.01$:**, $p \leq 0.05$:*] ($n = 3$)

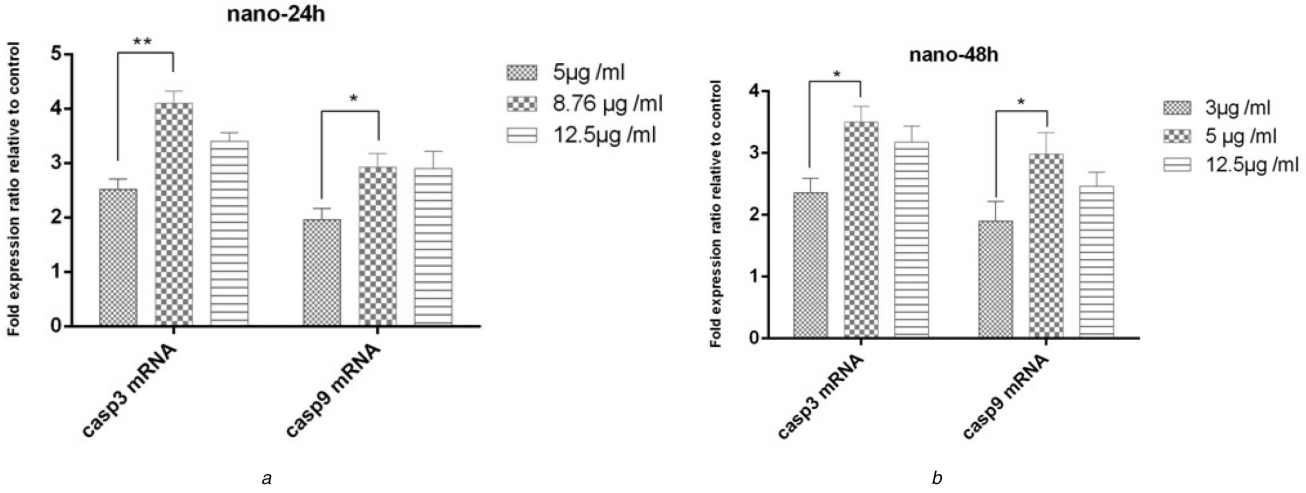


**Fig. 8** *Comparison of caspase 3 and 9 mRNA levels in MCF-7 cell lines*
***(a)*** After 24 h of treatment with biosynthesised nanoparticles ***(b)*** after 48 h

proliferation (93%), which was statistically significant ($P<0.001$), whereas the 3.0 µg/ml concentration showed the least anti-proliferative effect (18.5%). The $IC_{50}$ of the biosynthesised AgNPs was 8.76 and 5.0 µg/ml at 24 and 48 h, respectively. Flow cytometry analysis showed an increase in the apoptosis at all three concentrations of 5.0 µg/ml ($IC_{50}$), 8.76 µg/ml, and 12.5 µg/ml compared to the control group. The highest apoptosis was induced at $IC_{50}$ of nanoparticles, in a way that 31% more apoptosis induction was observed in cancer cells compared to the control group (untreated cells) *(*$P<0.001$). In addition, apoptosis was 3.5-fold higher than necrosis ($P<0.001$).

MCF-7 cells were treated with different concentrations of synthesised nanoparticles to investigate the mRNA expression of caspases 3 and 9 genes for 24 and 48 h. The treatment of MCF-7 cells at 5.0, 8.76 µg/ml ($IC_{50}$), and 12.5 µg/ml concentrations of nanoparticles for 24 h and 3.0, 5.0 µg/ml ($IC_{50}$), and 12.5 µ/ml concentrations for 48 h resulted in the up-regulation of expression of mRNAs of caspases 3 and 9 genes compared to the untreated cells. The highest mRNA expression of caspases was observed at the $IC_{50}$ of the nanoparticles (Fig. 7). The caspase 3 mRNA level was increased 4-fold, whereas the caspase 9 mRNA level increased 3.3-fold compared to the untreated cells in 24 h. A 3.5-fold increase in caspase 3 and 2.8-fold increase in caspase 9 mRNA expression was observed at 48 h compared to the control group. These data confirmed the pattern of induction of apoptosis by nanoparticles to be concentration and time-dependent.

The expression of caspase 3 and 9 genes in MCF-7 cell line at $IC_{50}$ of nanoparticles at 24 h was 1.6-fold higher than at 5.0 µg/ml, which was statistically significant ($P<0.01$).

However, the increase in the expression at $IC_{50}$ compared to 12.5 µg/ml concentration was not significant ($P>0.05$). In addition, the expression of caspase 3 and 9 genes in MCF-7 cells at $IC_{50}$ concentration of nanoparticles at 48 h was 1.5-fold higher than 3.0 µg/ml concentration, which was statistically significant ($P<0.01$). However, the increase the expression at $IC_{50}$ compared to 12.5 µg/ml concentration was not significant ($P>0.05$).

Vuong *et al.* [35] demonstrated that biologically synthesised AgNPs are predominantly in the spherical form with the average size in the range of 3–30 nm. They investigated the effects of various concentrations of AgNPs on growth, development and yield of peanut plants.

In 2017, Prasannaraj and Venkatachalam [36] synthesised spherical AgNPs with an average size of 40–90 nm using *C. asiatica*. The nanoparticles showed cytotoxic effects on the HepG2 and PC3 cell lines. The $IC_{50}$ value of the nanoparticles was 40.0 and 52.99 µg/ml for HepG2 and PC3 at 48 h, respectively.

Rout *et al.* and Logeswari *et al.* synthesised AgNPs with an average size of 30–50 and 42 nm using aqueous *C. asiatica* extract, respectively [37, 38].

It is noteworthy that the size of the synthesised nanoparticles in this study is smaller than that reported in similar studies, where nanoparticles were synthesised using the extract of *C. asiatica*.

The average in size of synthesised nanoparticles in this study was 19.17 nm, which is much less than that obtained in a study by Route *et al.* (30–50 nm), Logeswari *et al.* (42 nm) and by Prasannaraj and Venkatachalam (40–90 nm) [36–38]. Rout *et al.* and Logeswari *et al.* studied the effect of the synthesised

nanoparticles against human pathogens but not the anti-cancer activity of synthesised nanoparticles.

It worth to be noted that no cytotoxic, anti-proliferative effects and apoptosis induction were examined in those studies [36–38].

Therefore, this study is a new approach on the anti-cancer activity of nanoparticles synthesised by *C. asiatica*, and the expression of the intrinsic apoptosis pathway genes, including caspases 3 and 9 on MCF-7 cells.

With regard to the therapeutic potential of *C. asiatica*, the cytotoxic potential and anti-cancer effects of the nanoparticles, synthesised by this plant, on MCF-7 cells are compared with extract plant.

The inhibitory and anti-proliferative effects of asiaticoside, an active ingredient of *C. asiatica*, were observed in the MCF-7 cell line. The $IC_{50}$ of asiaticoside was estimated to be 40 µmol at 48 h. It was also shown that the activity of caspase 3 increases with the increasing concentration of asiaticoside [10].

In another study, the $IC_{50}$ of asiatic acid was measured to be 5.95 µmol in the MCF-7 breast cancer cell line. In this study, asiatic acid was shown to have no significant effect on the expression levels of caspase 8 and p53 genes but triggered the internal pathway of apoptosis, accompanied by the release of cytochrome C and increased expression of caspase 9 [11].

The effect of methanolic extract of *C. asiatica* as well as asiatic acid, one of the active compounds of this plant, on MCF-7, HEPG2, HeLa, and SW480 cell lines was studied by Babykutty *et al.* [9]. The results showed that the methanolic extract of the plant had a more inhibitory effect on MCF-7 line. The $LD_{50}$ (concentration at which a compound exhibits 50% lethality) for this compound was 66.0 µg, and the highest growth inhibition was reported at 82.0 µg, though asiatic acid showed 95% cell death at a concentration of 10 µmol.

In the previous studies, the toxic effect of *C. asiatica* extract or its active compounds on cancer cells has been shown, but the reports on the effect of synthesised nanoparticles, using *C. asiatica* extract, on the induction of cell apoptosis and the expression of genes associated with apoptosis, such as caspases 3 and 9, are not available.

By comparing the biosynthesised AgNPs with a mean size of 19.17 nm in this study and an $IC_{50}$ value (8.68 µg/ml) of synthesised nanoparticles compared with other studies, it appears that the method used in the present research have higher efficiency for the synthesis and a stronger antiproliferative effect against MCF-7 cancer cells compared to the mentioned studies. The size of nanoparticles synthesised in various studies was highly dependent on the type of method, genus, and plant species. In addition, the comparison of the effective concentration of different nanoparticles reported earlier with that reported in this study in preventing the growth of MCF-7 cancer cells shows that the synthesised nanoparticles in our study could induce cytotoxic and apoptotic effects with much less concentration, indicating the effective synthesis and stronger anti-proliferative abilities of the nanoparticles synthesised by *C. asiatica*. The results of this study confirmed and strengthened the observations of other studies on the role of nanoparticles in the activation of the apoptotic intrinsic pathway [11, 19, 36].

The results of this study suggest that the AgNPs, synthesised using *C. asiatica* extract, exert anti-proliferative activity through activation of cell death via the caspase-dependent intracellular pathway, as evident by increased activity of caspases 3 and 9.

## 5 Conclusion

This study emphasised the significance of the green synthesised AgNPs using *C. asiatica* leaf extract. The method could be considered to be an eco-friendly and cost-effective approach, characterised by the absence of a need to add any reducing and capping agents (commonly used in physicochemical synthesis) for the biosynthesis of nanoparticles. The benefits of this method include the speed of the reaction process, low cost, and easy access. In other words, green synthesised AgNPs, with an average size of 19.17 nm, possess the ability to inhibit cell proliferation and induce apoptosis in a manner that is dependent on the concentration and treatment time in MCF-7 cancer cells. This study is the first one to report these observations. Therefore, the synthesised nanoparticles, following the confirmation by supplementary tests and in vivo studies, can serve as a potential tool for cancer treatment.

## 6 Acknowledgments

The authors acknowledge the Islamic Azad University for contribution in this research.

## 7 References

[1] Rechinger, K.H.: Flora Iranica. (Umbelliferae). Akademische Druck-U. Verlagsanstalt. Graz _ Austria. 1978, p. 162

[2] Mozaffarian, V.: '*The family of umbelliferae in Iran (keys and distribution)*' (Research Institute of Forests and Rangelands Iran, Iran, Tehran, 1983), pp. 23–24

[3] Vaidya, A.D.B., Devasagayam, T.P.A.: 'Current status of herbal drugs in India: an overview', *J. Clin. Biochem. Nutr.*, 2007, **41**, pp. 1–11

[4] Jalili, A., Jamzad, Z.: '*Red data book of plant species of Iran*' (Research institute of forests and rangelands Tehran, Iran, Tehran, 1999), pp. 663–748

[5] Brinkhaus, B., Lindner, M., Schuppan, D., *et al.*: 'Chemical, pharmacological and clinical profile of the east Asian medical plant *Centella asiatica*', *Phytomedicine*, 2000, **7**, pp. 427–448

[6] Bonfill, M., Mangas, S., Cusido, R.M., *et al.*: 'Identification of triterpenoid compounds of *Centella asiatica* by thin layer chromatography and mass spectrometry', *Biomed. Chromatogr. A*, 2006, **742**, pp. 27–130

[7] Inamdar, P.K., Yeole, R.D., Ghogare, A.B., *et al.*: 'Determination of biologically active constituents in *Centella asiatica*', *J. Chromatogr. A*, 1996, **1**, p. 12

[8] Matsuda, H., Morikawa, T., Ueda, H., *et al.*: 'Medicinal foodstuffs, XXVI. Saponin constituents of gotu kola (2): structures of new ursane- and oleanane-type triterpene polyglycosides, *Centella saponins* B, C, and D, from *Centella asiatica* cultivated in Sri Lanka', *Chem. Pharm. Bull.*, 2001, **4**, pp. 1368–1371

[9] Babykutty, S., Padikkala, J., Sathiadevan, P.P., *et al.*: 'Apoptosis induction of *Centella asiatica* on human breast cancer cells', *Afr. J. Tradit. Complement. Altern. Med.*, 2008, **6**, pp. 9–16

[10] Al-Saeedi, F.J., Bitar, M., Pariyani, S.: 'Effect of asiaticoside on 99mTc-tetrofosmin and 99mTc-sestamibi uptake in MCF-7 cells', *J. Nucl. Med. Technol.*, 2011, **39**, pp. 279–283

[11] Ya-Ling, H., Po-Lin, K., Liang-Tzung, L.: 'Asiatic acid, a triterpene, induces apoptosis and cell cycle arrest through activation of extracellular signal-regulated kinase and p38 mitogen-activated protein kinase pathways in human breast cancer cells', *J. Pharmacol. Exp. Ther.*, 2005, **313**, pp. 333–344

[12] Zeichner, S.B., Ambrose, T., Zaravinos, J., *et al.*: 'Defining the survival benchmark for breast cancer patients with systemic relapse', *Breast Cancer (Auckl)*, 2015, **9**, pp. 9–17

[13] Kreyling, W.G., Semmler-Behnke, M., Chaudhry, Q.: 'A complementary definition of nanomaterial', *Nanotoday*, 2010, **5**, pp. 165–168

[14] El-Sayed, I.H., Huang, X., El-Sayed, M.A.: 'Surface plasmon resonance scattering and absorption of anti-EGFR antibody conjugated gold nanoparticles in cancer diagnostics: applications in oral cancer', *Nano Lett.*, 2005, **5**, pp. 829–834

[15] Elechiguerra, J.L., Burt, J.L., Morones, J.R., *et al.*: 'Interaction of silver nanoparticles with HIV-1', *J. Nanobiotechnol.*, 2005, **3**, p. 6

[16] Nagal, R., Singla, R.K.: 'Nanoparticles in different delivery systems: a brief review', *Indo Global J. Pharmaceut. Sci.*, 2013, **3**, pp. 96–106

[17] Lim, Y.Y., Murtijaya, J.: 'Antioxidant properties of *Phyllanthus amarus* extracts as affected by different drying methods', *LWT Food Sci. Technol.*, 2007, **40**, pp. 1664–1669

[18] Sathishkumar, M., Sneha, K., Won, S.W., *et al.*: 'Cinnamonzeylanicum bark extract and powder mediated green synthesis of nano-crystalline silver particles and its bactericidal activity', *Colloids Surf. B Biointerfaces*, 2009, **73**, pp. 332–338

[19] Mousavi, B., Tafvizi, F., Zaker Bostanabad, S.: 'Green synthesis of silver nanoparticles using *Artemisia turcomanica* leaf extract and the study of anti-cancer effect and apoptosis induction on gastric cancer cell line (AGS)', *Artif. Cells. Nanomed. Biotechnol.*, 2018, **23**, pp. 1–12. [oEpub ahead of print]

[20] Iravani, S., Korbekandi, H., Mirmohammadi, S.V., *et al.*: 'Synthesis of silver nanoparticles: chemical, physical and biological methods', *Res. Pharm. Sci.*, 2014, **9**, pp. 385–406

[21] Sharma, N.C., Sahi, S.V., Nath, S., *et al.*: 'Synthesis of plant-mediated gold nanoparticles and catalytic role of biomatrix-embedded nanomaterials', *Environ. Sci. Technol.*, 2007, **41**, pp. 5137–5142

[22] Jacob, S.J., Finub, J.S., Narayanan, A.: 'Synthesis of silver nanoparticles using *Piper longum* leaf extracts and its cytotoxic activity against Hep-2 cell line', *Colloids Surf. B Biointerfaces*, 2012, **91**, pp. 212–214

[23] Arunachalam, R., Dhanasingh, S., Kalimuthu, B., *et al.*: 'Phytosynthesis synthesis of silver nanoparticles using *Coccinia grandis* leaf extract and its application in the photocatalytic degradation', *Colloids Surf. B Biointerfaces*, 2012, **94**, pp. 226–230

[24] Raghunandan, D., Ravishankar, B., Sharanbasava, G., *et al.*: 'Anti-cancer studies of noble metal nanoparticles synthesized using different plant extracts', *Cancer Nanotechnol.*, 2011, **2**, pp. 57–65

[25] Daizy, P.: 'Green synthesis of gold and silver nanoparticles using *Hibiscus rosa*', *Physica E*, 2010, **42**, pp. 1417–1424

[26] Priya, R.S., Geetha, D., Ramesh, P.S.: 'Antioxidant activity of chemically synthesized AgNPs and biosynthesized *Pongamia pinnata* leaf extract

mediated AgNPs – a comparative study', *Ecotoxicol. Environ. Saf.*, 2016, **134**, pp. 308–318
[27] Derfus, A.M., Chan, W.C.W., Bhatia, S.N.: 'Intracellular delivery of quantum dots for live cell labeling and organelle tracking', *Adv. Mater.*, 2004, **16**, pp. 961–966
[28] Xia, T., Kovochich, M., Brant, J., *et al.*: 'Comparison of the abilities of ambient and manufactured nanoparticles to induce cellular toxicity according to an oxidative stress paradigm', *Nano Lett.*, 2006, **6**, pp. 1794–1807
[29] Carlson, C., Hussain, S.M., Schrand, A.M., *et al.*: 'Unique cellular interaction of silver nanoparticles: size dependent generation of reactive oxygen species', *J. Phys. Chem. B*, 2008, **112**, pp. 13608–13619
[30] Xia, T., Kovochich, M., Liong, M., *et al.*: 'Comparison of the mechanism of toxicity of zinc oxide and cerium oxide nanoparticles based on dissolution and oxidative stress properties', *ACS Nano*, 2008, **2**, pp. 2121–2134. 39
[31] Saptarshi, S.R., Duschl, A., Lopata, A.L.: 'Interaction of nanoparticles with proteins: relation to bio-reactivity of the nanoparticle', *J. Nanobiotech.*, 2013, **11**, p. 26
[32] Rahban, M., Divsalar, A., Saboury, A.A., *et al.*: 'Nanotoxicity and spectroscopy studies of silver nanoparticle: calf thymus DNA and K562 as targets', *J. Phys. Chem. C*, 2010, **114**, pp. 5798–5803
[33] Lu, W., Senapati, D., Wang, S., *et al.*: 'Effect of surface coating on the toxicity of silver nanomaterials on human skin keratinocytes', *Chem. Phys. Lett.*, 2010, **487**, pp. 92–96
[34] Hsin, Y.H., Chen, C.F., Huang, S., *et al.*: 'The apoptotic effect of nanosilver is mediated by a ROS- and JNK-dependent mechanism involving the mitochondrial pathway in NIH3T3 cells', *Toxicol. Lett.*, 2008, **179**, pp. 130–139
[35] Vuong, L.D., Luan, N.D.T., Ngoc, D.D.H., *et al.*: 'Green synthesis of silver nanoparticles from fresh leaf extract of *Centella asiatica* and their applications', *Int. J. Nanosci.*, 2017, **16**, p. 1650018
[36] Prasannaraj, G., Venkatachalam, P.: 'Green engineering of biomolecule-coated metallic silver nanoparticles and their potential cytotoxic activity against cancer cell lines', *Adv. Nat. Sci., Nanosci. Nanotechnol.*, 2017, **8**, p. 025001
[37] Rout, A., Kumar, J.P., Kumar, P.U., *et al.*: 'Green synthesis of silver nanoparticles using leaves extract of *Centella asiatica* for studies against human pathogens', *Int. J. Pharma. Bio. Sci.*, 2013, **4**, pp. 661–674
[38] Logeswari, P., Silambarasan, S., Abraham, J.: 'Eco friendly synthesis of silver nanoparticles from commercially available plant powders and their antibacterial properties', *Scientia Iranica*, 2013, **20**, pp. 1049–1054